 DOI: 10.1109/IGARSS47720.2021.9553195

A PRE-CORRELATION RFI MITIGATION ALGORITHM FOR L-BAND INTERFEROMETRIC RADIOMETERS

[1,3]*J. Querol,* [2,3]*A. Camps,* [2, 3]*A. Pérez,* [4]*R. Oliva,* [4]*R. Onrubia,* [5]*J. I. Ramirez-Martinez,* [5]*A. Zurita,* [6]*M. Suess,* [6]*M. Martin-Neira*

[1]Interdisciplinary Centre for Security Reliability and Trust (SnT), University of Luxembourg
[2]Unidad María de Maeztu CommSensLab-UPC – Dept. of Signal Theory and Communications, Universitat Politècnica de Catalunya-BarcelonaTech and IEEC/CTE-UPC
[3]MITIC Solutions S.L.
[4]Zenithal Blue Technologies S.L.U.
[5]Airbus Defence and Space S.A.U.
[6]European Space Research and Technology Centre (ESTEC), European Space Agency (ESA)

E-mail: jorge.querol@uni.lu, camps@tsc.upc.edu, adrian.perez.portero@upc.edu, r.oliva@zenithalblue.com, onrubia@zenithalblue.com, juanignacio.ramirez@airbus.com, alberto.zurita@airbus.com, martin.suess@esa.int, manuel.martin-neira@esa.int

ABSTRACT

Radio Frequency Interference (RFI) is a major concern for both real and synthetic aperture radiometers. After the lessons learnt from SMOS, ESA is preparing the next-generation of L-band interferometric radiometers with RFI mitigation integrated in the cross-correlators. This work presents a preliminary design and results of a pre-correlation RFI mitigation algorithm tailored for interferometric radiometers. The results show that the correlation error introduced by the RFI is reduced on average to the half, with peaks of 20 dB of mitigation.

Index Terms— Interferometric radiometer, RFI, mitigation

1. INTRODUCTION

Radio-Frequency Interference (RFI) signals are undesired electromagnetic emissions that can degrade the performance of any receiver. Nowadays, the concern about the RFI phenomenon is increasing due to the high number of RFI occurrences detected, and this problem is expected to grow even more in the future because of the pervasive use and abuse of wireless technologies around the world. RFI signals are either those illegally emitted at bands reserved for passive observations (in-band emissions), or those that are legally emitted in adjacent bands, but a fraction of their power leaks into the bandwidth of the receiver (near-band emissions), or even a harmonic emission at a much lower frequency band that falls in the pass-band. The origin of these RFI signals can be of very different nature. RFI can be intentional or unintentional, and it can be generated externally or even by the same device, although these last ones must be minimized by proper design. They can be lower harmonics, inter-modulation products, out-of-band emissions, or even intentional emissions designed to override a particular frequency band. As pointed in [1], the allocated bands provide a statutory protection, with no guarantees against interference occurrences from accidental out-of-band emissions to intentional jamming.

RFI signals disrupt all types of microwave radiometers. The most common distinction between types of radiometers is their antenna configuration. Real aperture radiometers use a single antenna, whereas synthetic aperture radiometers have an interferometric array of antennas. The different antenna configuration distinguishes between the RFI mitigation techniques for real aperture, and afterwards, extends them to the more complex case of synthetic aperture [2].

Synthetic aperture radiometers refer to those that use multiple small antennas and interferometric signal processing (basically the complex cross-correlation of the signals collected by each pair of antennas) to obtain the resolution of a single large antenna. The synthetic aperture approach overcomes the barriers that the physical size of the antenna places on passive microwave remote sensing from space, as it replaces an unrealistically large antenna with an array of small antennas, eventually even in different platforms.

SMOS is ESA's Soil Moisture and Ocean Salinity mission, the second Earth Explorer mission. A description of this mission and its scientific achievements can be found in [3] and [4]. SMOS, launched in November 2009, has

exceeded already its extended lifetime of 3 years, and hence, ESA started several activities to prepare the technology for a future follow-on mission on L-band radiometry.

Even though SMOS operates in a frequency band reserved exclusively for passive microwave radiometry, a large number of illegal emissions in this frequency band that are disturbing the measurements have been observed since its launching [5]. Based on the SMOS experience, it is intended that RFI mitigation techniques are developed as part of the on-board correlator. The baseband signals sensed by the individual receivers and transmitted through the optical harness are cross-correlated in the correlator unit and integrated during the duration of one snapshot. Through this integration the data volume of the visibilities is greatly reduced compared to the one of the baseband signals, but the whole visibility measurement may be contaminated by RFI, even if the interference had only a very short duration or if it affected only a part of the signal spectrum.

This paper describes the first iteration of the RFI mitigation algorithm proposed for the next generation of ESA L-band interferometric radiometers.

2. ALGORITHM DESCRIPTION

The proposed RFI mitigation algorithm receives the signal from each one of the receivers and processes it independently. The digital signal is already filtered and quantized to 1-bit. The objective of the RFI mitigation signal is to eliminate the interfering signal as much as possible without significantly degrading the performance of the radiometer. The mitigated signal is delivered to the correlation block, where the signals coming from different receivers are cross-correlated. Fig. 1 shows the overall block diagram of the proposed RFI mitigation algorithm.

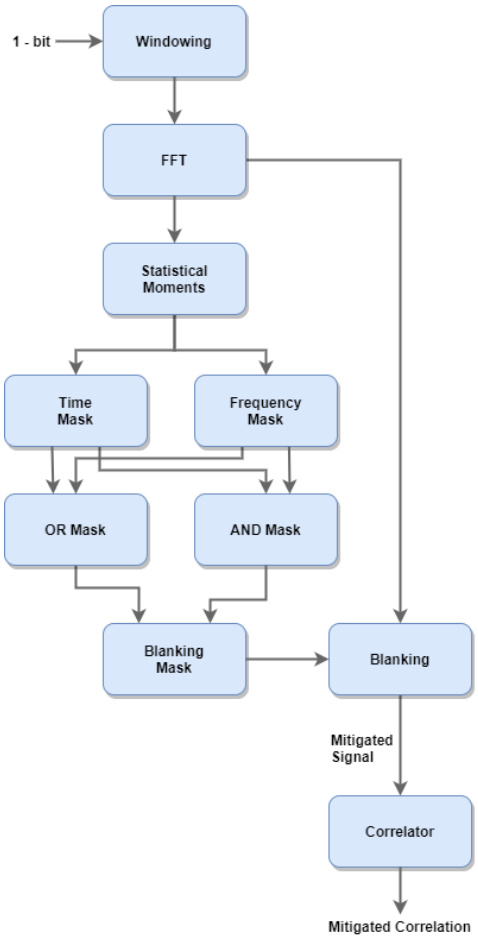

Fig. 1: Overall block diagram of the proposed RFI mitigation algorithm.

After an initial windowing to reduce the Gibbs effect associated to the truncation of the data streams, a Fast Fourier Transform (FFT) is evaluated to create a spectrogram of the input signal. The choice of the Hamming as the window function is a good trade-off between the spectral leakage in the frequency-domain and the length of the temporal response. The spectrogram is the most used technique for RFI excision and can be implemented in situations that require low power and small form factor devices. This approach can adapt rapidly to changing environments [6]. The signal is filtered in the time-frequency space to remove the RFI components before being transformed back to the time-domain.

After the spectrogram computation, the statistical moments are calculated simultaneously in the time and frequency domains to detect the presence of RFI. The selected statistical moment is the Kurtosis, which shows an outstanding performance considering its simple implementation [7]. When the Kurtosis is applied in a single frequency bin, it is coined as Spectral Kurtosis, whereas when it is applied for a single time bin is coined as Cross-frequency Kurtosis. The result of both approaches is compared to a particular threshold calculated according to a Constant False Alarm Rate (CFAR). The CFAR has been set to values a low as 10^{-8} to preserve the radiometric signal in case no RFI is present [8]. It is worth to mention that in synthetic aperture radiometers a second stage of RFI mitigation can still be performed in the imaging process as in [9], which does not apply in real aperture radiometers.

When RFI is detected in one of these domains, a blanking mask is calculated for both the time and frequency domains. These blanking masks can be combined in two ways: the bins are marked to be blanked if an RFI is detected either in time or frequency domain (OR mask), or when both domains detect the RFI simultaneously (AND mask). The AND mask (less aggressive) is selected by default, whereas the OR mask is only selected when no bin is marked with the AND approach.

Eventually, the selected blanking mask is applied to the spectrogram of the radiometric signal before it is delivered to the correlator. Fig. 2 shows an example of the application of the blanking masks on the spectrogram.

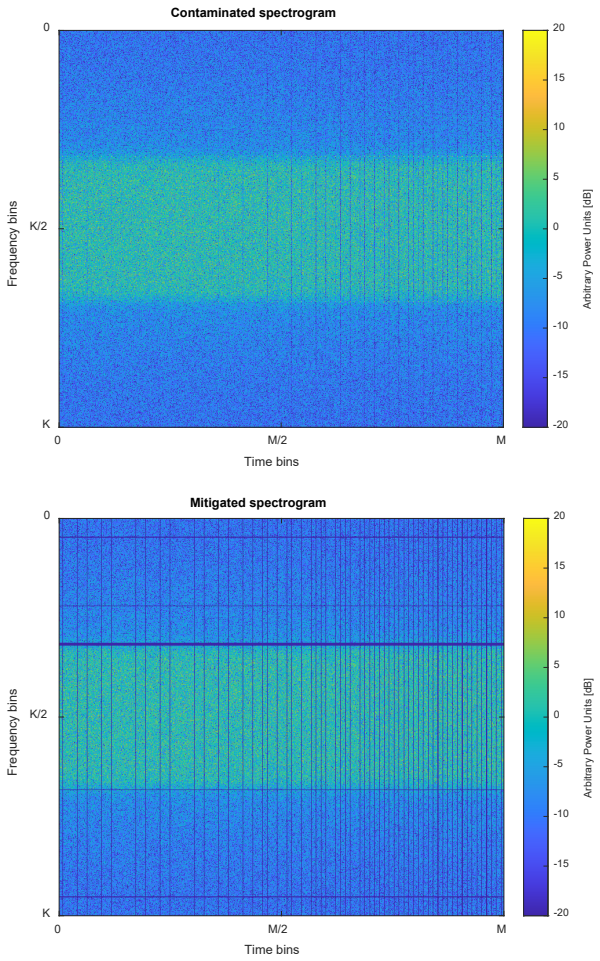

Fig. 2: Sample spectrogram before (top) and after (bottom) applying the corresponding blanking mask.

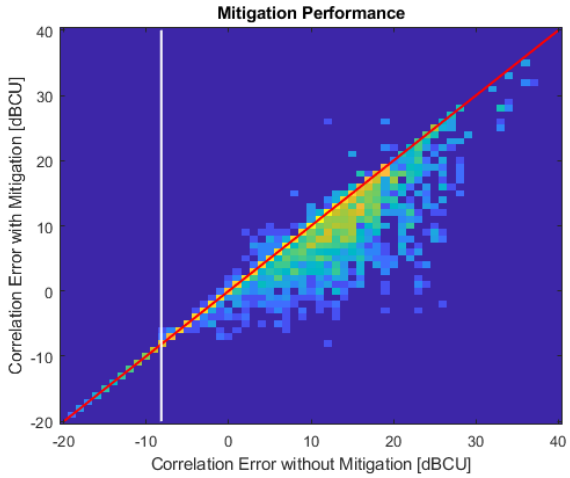

Fig. 3: Mitigation performance.

3. SIMULATION ENVIRONMENT

The RFI mitigation algorithm has been tested by running 1200 Monte-Carlo simulations with 3 different receivers and 6 different types of RFI signals: pulsed, CW, QPSK, FSK, QAM and chirp.

The time epochs are 200 ms long and the radiometric bandwidth is of 27 MHz. The sampling rate is set to 57.69375 MHz and the size of the FFT to 1024 samples. Thus, the number of frequency bins K is 1024, and the number of time bins M within an integration epoch is 22536.

The scenario generation has been created as close as possible to the RFI scenario suffered by SMOS. It is worth to mention that the power level of the RFI signals under simulation is much weaker than in a case with a highly directive real aperture radiometer such as SMAP, and hence, making the RFI detection process harder in the pre-correlation stage.

4. PRELIMINARY RESULTS

The mitigation performance of the proposed algorithm is evaluated by comparing the output value of the correlator with and without applying the mitigation. Since the magnitude of the output of the correlator depends on the radiometric scenario itself, the correlation error introduced by the RFI is defined as a figure of merit for a fair comparison among the results. Thus, the correlation error without mitigation is defined as

$$\epsilon_{cont} = 10^4 \cdot |corr_{Cont} - corr_{clean}|, \qquad (1)$$

where $corr_{cont}$ is the output of the correlator without mitigation (only signal contaminated with RFI), and the correlation error with mitigation is defined as

$$\epsilon_{mit} = 10^4 \cdot |corr_{mit} - corr_{clean}|, \qquad (2)$$

where $corr_{mit}$ is the output of the correlator with mitigation. The 10^4 factor has been added to express the magnitude of the correlation in the same Correlation Units (CU) used in SMOS.

Fig. 3 depicts the mitigation performance of the proposed algorithm for all the scenarios under consideration and all the cross-polarization combinations. The magnitude of the correlation errors is expressed in logarithmic units for a better representation ($40\ dBCU = 10 \cdot log(10^4 CU)$). The red line defines the unitary slope line. The results located under the red line show actual error reduction or mitigation, whereas the ones above correspond to a degradation of the measurements. The design of any mitigation algorithm

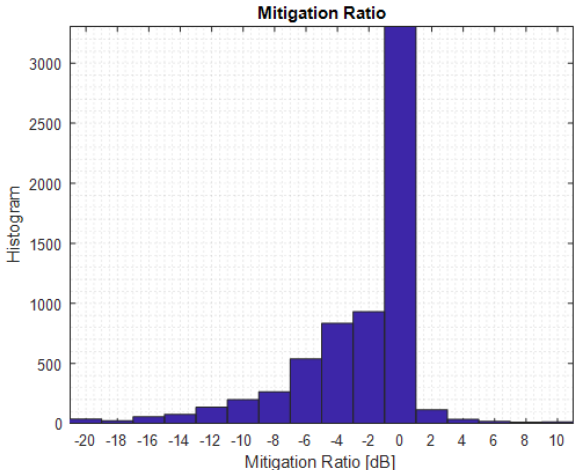

Fig. 4: Mitigation ratio histogram.

should maximize the former while minimizing the latter. The vertical white line is located at -8.16 dBCU corresponding to a 16-bit quantization noise floor. Hence, error values located at the left of white line are masked by the quantization floor.

The mitigation performance can be further expressed as the ratio of the correlation errors as

$$\rho_{mit} = \frac{\epsilon_{mit}}{\epsilon_{cont}}, \quad (3)$$

coined as the correlation ratio. Fig. 4 shows a histogram of the mitigation ratio in dB units. This representation allows to better quantify the mitigation performance.

The results show that the algorithm is performing well in the 57.6% of the cases, and it is degrading only in the 5.5% of the cases. These results are difficult to compare with previous results, but one can take as a reference the constant false alarm rate from real aperture radiometers such as SMAP (9.3%) [10]. It is also worth to mention that the given the design of the algorithm, no false alarm was detected during the simulations.

The mean mitigation ratio considering all the cases is -3 dB. Therefore, the correlation error introduced by the RFI signal is reduced to the half in average, however, in some cases the mitigation reaches more than -20 dB. Table 1 summarizes the obtained results.

5. CONCLUSIONS

This paper describes the preliminary design and results of a pre-correlation RFI mitigation algorithm for interferometric radiometers. The results show that the correlation error introduced by the RFI is reduced to the half, with performance peaks of 20 dB of mitigation.

Table 1: Summary of mitigation ratio results.

All	Mitigating (<0)	Degrading (>0)
Mean -3,0 dB Best < -20 dB	%. It. 57,6% Mean -4.2 dB	%. It. 5,5% Mean 1.5 dB

REFERENCES

[1] A. J. Gasiewski, M. Klein, A. Yevgrafov and V. Leuskiy, "Interference mitigation in passive microwave radiometry," IEEE International Geoscience and Remote Sensing Symposium, Toronto, Ontario, Canada, 2002, pp. 1682-1684 vol.3, doi: 10.1109/IGARSS.2002.1026220.

[2] J. Querol, A. Perez, and A. Camps, "A Review of RFI Mitigation Techniques in Microwave Radiometry," Remote Sensing, vol. 11, no. 24, p. 3042, Dec. 2019, doi: 10.3390/rs11243042.

[3] Y. H. Kerr et al., "The SMOS Mission: New Tool for Monitoring Key Elements of the Global Water Cycle," in Proceedings of the IEEE, vol. 98, no. 5, pp. 666-687, May 2010, doi: 10.1109/JPROC.2010.2043032.

[4] J. Font et al., "SMOS: The Challenging Sea Surface Salinity Measurement From Space," in Proceedings of the IEEE, vol. 98, no. 5, pp. 649-665, May 2010, doi: 10.1109/JPROC.2009.2033096.

[5] R. Oliva et al., "SMOS Radio Frequency Interference Scenario: Status and Actions Taken to Improve the RFI Environment in the 1400–1427-MHz Passive Band," in IEEE Transactions on Geoscience and Remote Sensing, vol. 50, no. 5, pp. 1427-1439, May 2012, doi: 10.1109/TGRS.2012.2182775.

[6] J. M. Tarongi and A. Camps, "Radio frequency interference detection and mitigation algorithms based on spectrogram analysis", Algorithms, vol. 4, no. 4, pp. 239-261, 2011, doi: 10.3390/a4040239.

[7] J. M. Tarongi and A. Camps, "Normality analysis for RFI detection in microwave radiometry", Remote Sens., vol. 2, no. 1, pp. 191-210, Dec. 2009, doi: 10.3390/rs2010191.

[8] J. Querol, R. Onrubia, A. Alonso-Arroyo, D. Pascual, H. Park and A. Camps, "Performance Assessment of Time–Frequency RFI Mitigation Techniques in Microwave Radiometry," in IEEE Journal of Selected Topics in Applied Earth Observations and Remote Sensing, vol. 10, no. 7, pp. 3096-3106, July 2017, doi: 10.1109/JSTARS.2017.2654541.

[9] Camps, A.; Gourrion, J.; Tarongi, J.M.; Vall Llossera, M.; Gutierrez, A.; Barbosa, J.; Castro, R. Radio-Frequency Interference Detection and Mitigation Algorithms for Synthetic Aperture Radiometers. Algorithms 2011, 4, 155-182, doi: 10.3390/a4030155.

[10] J. R. Piepmeier et al., "Radio-Frequency Interference Mitigation for the Soil Moisture Active Passive Microwave Radiometer," in IEEE Transactions on Geoscience and Remote Sensing, vol. 52, no. 1, pp. 761-775, Jan. 2014, doi: 10.1109/TGRS.2013.2281266.